

Conduction and Inertia Correction for Transient Thermocouple Measurements. Part II: Experimental Validation and Application

Tobias Krille*, Rico Poser, Markus Diel, and Jens von Wolfersdorf

Institute of Aerospace Thermodynamics (ITLR), University of Stuttgart, 70569, Stuttgart, Germany

Abstract. Thermocouples are often used for temperature measurements. Under transient conditions, measurement errors can occur due to capacitive inertia and heat conduction along the stem of the thermocouples. To correct such errors, a method is presented in Part I [1] of this paper, which uses a simplified analytical approach and a numerical solution. In the present work, this method is applied to temperature measurements. Several experiments with different thermocouple designs were performed to investigate different conditions such as installation depth, thermocouple type and transient temperature rises. In all cases, two thermocouples were placed so that they are exposed to the same fluid temperature. They are installed with short or long immersion length, respectively. It is shown that only the short thermocouple experiences a thermal conduction error, but both are subject to thermal inertia. The importance of compensating for these effects is shown by quantifying the errors in a typical heat transfer experiment when they are neglected. It is shown, which parameters are necessary for a re-calculation of fluid temperatures when two thermocouples are present at the same measuring position. Furthermore, a simplified method is described, which can be applied if the instrumentation of only one thermocouple is possible.

1 Nomenclature

A	m^2	area
c	$J\ kg^{-1}\ K^{-1}$	specific heat capacity
D	m	diameter
e	–	error
h	$W\ m^{-2}\ K^{-1}$	heat transfer coefficient
k	$W\ m^{-1}\ K^{-1}$	thermal conductivity
L	m	immersion length
\dot{m}	$kg\ s^{-1}$	mass flow rate
Pr	–	Prandtl number
Q	J	heat
Re	–	Reynolds number
T	K	temperature
t	s	time
V	m^3	volume
y	m	lateral coordinate

Greek symbols

Δ	–	difference
η	$kg\ m^{-1}\ s^{-1}$	viscosity
θ	–	dimensionless temperature
ρ	$kg\ m^{-3}$	density
τ	s	time constant

Subscripts

0	initial condition
ave	average
c	cross-section
eff	effective
est	estimated

f	fluid
ref	reference
TC	thermocouple
tip	thermocouple tip
w	wall

2 Introduction

Thermocouples are the most commonly used measuring device for local temperatures and for the determination of the heat transfer rate. In such experiments, but also in many other application fields where thermal behavior is analyzed, precise temperature measurement is crucial for accurate results. Thermocouples measure the temperature at their tip, where two metallic wires are welded together generating a temperature-dependent voltage due to the Seebeck effect.

However, when the measurement tip and the thermocouple stem are at different temperatures, heat conduction along the metal pair occurs. This difference produces a sensor reading that is different from the actual heat source temperature and is referred to as the stem effect. Under transient conditions, capacitive inertia effects have to be considered as well as they will cause time delays in the temperature reading. In transient heat transfer experiments, a temperature jump is often applied to the fluid temperature while the temperature response of the wall is observed. Measurement errors will occur when the inertia error is

* Corresponding author: tobias.krille@itlr.uni-stuttgart.de

neglected, especially in fast experiments. The true fluid temperature can be re-calculated by [2]

$$T(t) = T_{TC}(t) + \tau_{TC} \frac{\Delta T_{TC}}{\Delta t}, \quad (1)$$

where T is the true fluid temperature and T_{TC} is the temperature measured by the thermocouple. The time constant τ_{TC} is calculated by

$$\tau_{TC} = \frac{\rho_{tip} c_{tip} V_{tip}}{h A_{tip}}. \quad (2)$$

Here, besides the geometrical information V and A the material properties ρ and c , also the heat transfer coefficient h at the thermocouple tip needs to be known, which in most cases only can be approximated by correlations. While inertia errors become minor with long test times, heat conduction errors remain even if an almost stationary state is reached in the temperature field. Such errors due to conduction along the thermocouple sheath are not trivial to determine. In [3] the relative stem conduction error is conservatively estimated to be

$$\theta_{est} = 1 - \frac{T_{TC} - T_0}{T_f - T_0} = e^{-\frac{L}{D_{eff}}} \quad (3)$$

with D_{eff} being the effective diameter of the thermocouple tip. For a thermocouple with sheathed tip it can be calculated by

$$D_{eff} = \sqrt{\frac{k D_{tip}}{4 h}}. \quad (4)$$

Again, only a rough estimation of these errors is possible and the outcome of Eq. (3) strongly depends on the heat transfer coefficient on the thermocouple tip. Nevertheless, this relationship can be used to estimate the minimal immersion depth of the thermocouples in order to neglect stem effect errors.

Axtmann et al. [4] showed that the measured fluid temperature strongly depends on the installation situation of the thermocouples (see Fig. 1). In a symmetrical channel, they measured the temperature profile with thermocouples traversed from one channel wall to the opposite. The expected symmetrical temperature field only was measured, when the thermocouple root was heated at the same level as the fluid temperature.

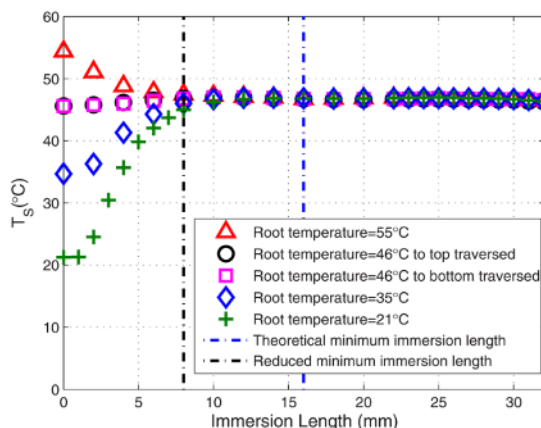


Fig. 1. Impact of root temperature on measured temperature. (Axtmann et al. [4])

It can be said that stem effect errors can be reduced by controlling the thermocouple root or increasing the installation depth (e.g. by buckling the thermocouple). However, in small experimental geometries, it can be impossible to reach the minimum required immersion length. Controlling the root and buckling the thermocouples can be inapplicable too.

Under such conditions, it is necessary to correct the temperature measurement afterwards. Therefore, a model is needed, that allows compensating conduction errors and thermal inertia at the same time.

In the present section of this two-part paper, temperature measurements are performed, which provide the foundation for the validation of the compensation method described in Part I [1]. Two thermocouples with short and long immersion lengths are exposed to the same fluid temperature history. The long thermocouple is intended to measure the temperature of the fluid without experiencing a stem conduction error. As all used thermocouples are similar, they will experience the same thermal inertia effects.

First, the experimental test series are presented that investigate the repeatability of the measurements as well as the influence of thermocouple type and temperature change on the stem effect. Then, the necessary input parameters to apply the numerical analysis are described, before the results are discussed. It will be shown that the method is suitable for re-calculating the true fluid temperatures from temperature measurements, which are subject to inertia and stem effects.

3 Experimental Setup and Procedure

Experiments are performed on the test rig shown in Fig. 2, which is basically the same as used by Axtmann et al. [4]. Only the Perspex model is replaced by a model with similar dimensions but a different cooling configuration. Details about this Perspex model can be found in [5].

In the present work, the plenum region of the Perspex model will be of interest. It has a relative large aspect ratio of 15.5, as the width is 201.5 mm while it is only 13 mm high. This can be leveraged to install thermocouples with both high and low immersion lengths that are exposed to the same fluid temperature. Four thermocouples are used in the experiments, two of type K and of type T, respectively. As shown in Fig. 3, two thermocouples are installed from the bottom and two from the sidewall. One thermocouple pair on each side of the plenum is supposed to measure at the same position. Therefore, the thermocouple tips are positioned manually so that they are as close as possible but still without touching each other. During instrumentation, care was taken to ensure that a gap between them is still visible.

The temperature measurement locations are 6.5 mm from the bottom (half the plenum height) and 61.75 mm from the sidewalls. As the thermocouples are installed straight through the walls, the named wall distances are also the respective immersion lengths. The bottom thermocouples are glued into the 20 mm thick Perspex walls. In contrast, the long thermocouples are

fixed by screw connections at the sidewalls of 13.5 mm thickness. In a later setup also at the bottom, thermocouple screw connections are used.

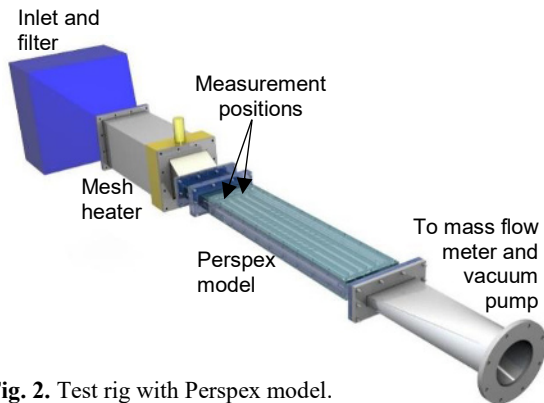


Fig. 2. Test rig with Perspex model.

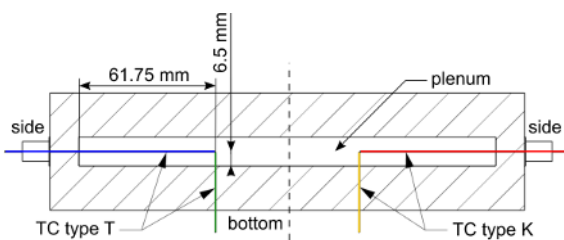


Fig. 3. Thermocouple installation details.

All used thermocouples are non-grounded with a 0.5 mm diameter sheath of Inconel 600. The two thermal shanks are surrounded by an insulation layer of magnesium oxide (MgO). The shanks are made of Alumel (Ni) and Chromel (NiCr) for type K and copper (Cu) and Constantan (CuNi) for type T thermocouples. Figure 4 shows the sectional view of a thermocouple and the material properties of the specific layers are listed in Tab. 1. Many researches worked on thermocouples and listed the typical shank material properties before [2, 6–13]. In this work, for each property a reasonable value, which is approximately the median of all references, is chosen.

The used properties for Inconel 600 and magnesium oxide are taken from a single data sheet source, respectively [14, 15]. Especially the thermal conductivity $k = 42 \text{ W/(m K)}$ of MgO must be considered with caution. The values found in literature vary between 0.6 W/(m K) [3] and 55.3 W/(m K) [16]. It strongly depends on the fact if MgO is present in crystalline or powder form. Powder has a much lower conductivity. However, the powder used in the thermocouples is highly compressed and multiple times rolled. The selected value, which describes the crystalline form delivered reasonable results.

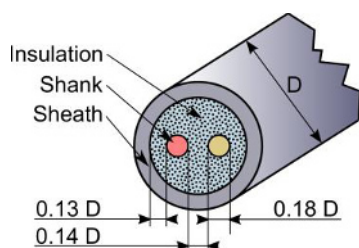


Fig. 4. Sectional view of a thermocouple.

Tab. 1. Properties of thermocouple materials.

	ρ (kg/m ³)	c (J/kg K)	k (W/m K)
Inconel 600	8470	444	15
MgO	3580	877	42
Ni (K)	8730	448	19
NiCr (K)	8600	530	30
Cu (T)	8900	383	386
CuNi (T)	8900	410	22

Table 2 shows the homogenized properties of the used thermocouple types K and T. The homogenized values of ρ and c were calculated by averaging the individual material values from Tab. 1 in relation to their mass fraction. In case of k the individual values are weighted according to their area proportion.

Tab. 2. Homogenized properties of thermocouples types K and T.

Property	Type K	Type T
D (mm)	0.5	0.5
ρ (kg/m ³)	5975	5990
c (J/kg K)	578	572
k (W/m K)	29.5	41.1

All temperatures are sampled at a frequency of 10 Hz. Before the experiment they were calibrated in an isothermal dry block with an accuracy of $\pm 0.1^\circ\text{C}$.

To generate a mass flow, air is sucked in through a filter by a vacuum pump. The mass flow rate through the model is measured by a laminar flow meter and can be adjusted by setting the position of a bypass valve. The flow conditions at the thermocouples will be described by the Reynolds numbers calculated as

$$\text{Re} = \frac{\dot{m} D}{A \eta(T)} \quad (5)$$

The thermocouple diameter is chosen as reference length and the temperatures dependence of the fluid's viscosity is considered.

In front of the Perspex model, an electrical mesh heater is positioned, that enables rapidly heating the fluid before it enters the test section. By that, a steep rise in the fluid temperature can be realized.

Before each experiment, the Perspex model and the fluid are in thermal equilibrium and a constant mass flow rate is set. Activating the heater with presumably set heating power indicates the start of each experimental run. The heater is active for at least 20 seconds and is then turned off again.

Before the numerical analysis is applied, only the temperatures at the start and at the end of an experiment are regarded. As detailed described in Part I [1] of this paper, the measurement error due to thermal inertia occurs only at the beginning of the experiments, whereas the stem effect also occurs in steady state. After 20 s the measured temperature curves are regarded to be steady. As the immersion length of the long thermocouples is high, they are assumed to experience no stem effect and measure the true fluid temperature instead. The stem effect of the short thermocouple will be defined as the difference ΔT between the measured temperatures of the long and the short thermocouple at the end of the experiment.

$$\Delta T = |T_{TC, long} - T_{TC, short}| \quad (6)$$

To compare different setting without the influence of changing initial temperatures or the size of the temperature step, the results are also presented in the dimensionless form

$$\theta = \frac{\Delta T}{T_{max} - T_0} \quad (7)$$

where T_{max} and T_0 are the average temperatures after 20 seconds and before the start of an experiment, respectively. The mean value was always calculated from five consecutive samples. θ is the dimensionless temperature difference measured by the short and long thermocouple in relation to the fluid temperature step and can be interpreted as measurement error caused by the stem effect.

4 Experimental Results

Several experiments were performed to measure the stem effect of the short thermocouples.

First, the influence of the thermocouple type shall be discussed. This can be done for every experimental run, as thermocouple type K and T are always used at the same time. Besides the thermocouple type, also the repeatability of the measurements is investigated. Therefore, multiple experiments are performed under the same conditions with either identical or similar setup. The latter is achieved by removing and reinstalling the same thermocouples or replacing them by thermocouples of the same type and production charge. An additional set of experiments is conducted to investigate the influence of the temperature step size.

Figure 5 shows the temperature curves of the four installed thermocouples of an exemplary experiment. However, as previously described, for evaluating the stem effect of the short thermocouples only the differences between the start and end temperatures are required. All transient behavior will be subject to the last part of the paper when the results of the numerical simulation are introduced. The temperatures at start and end as well as all results of the discussed experiments are listed in Tab. 3. The Reynolds number is an average over the experimental duration of 20 s.

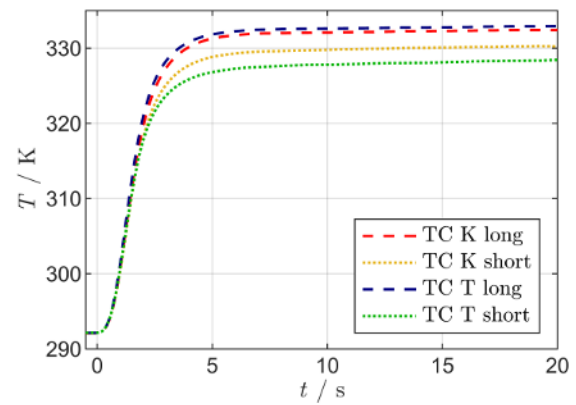


Fig. 5. Exemplary temperature curves of different thermocouples, T40-A1.

4.1 Variation of thermocouple type

Without discussing each of the experiments in detail, some first conclusions can be drawn by comparing the values of θ in Tab. 3. The measurement error is listed for both thermocouple types. In all experiments that were conducted, the error of short thermocouple type T is higher than that of type K. The error of type T ranges from 10.4% to 11.7%, while it is between 5.3% and 6.2% for type K. These differences result from the material composition of the respective thermocouples. As shown in Tab. 2, the effective thermal conductivity of type T thermocouples is about 1.4 times higher, which is due the high conductivity of copper.

4.2 Repeatability of Experiments

To assess if the results are the same, when an experiment is conducted several times, experiments named T40-A1, T40-A1* and T40-A1** are evaluated. Between these experiments, the thermocouple instrumentation was not changed. The test rig ran for at least one hour under ambient temperatures to reach an isothermal state before each experiment was conducted. As the ambient temperature slowly increased over the day, the starting conditions slightly changed. Nevertheless, θ differs only by 0.1% between the experiments. Higher differences are found, when the thermocouples are disassembled and remounted between two runs. This was done in the experiments named T40-A1, T40-A2 and T40-A3. The measured stem effect changes by about 1%. Similar results are obtained, when the thermocouples are exchanged by

Tab. 3. Results of temperature measurements.

Exp. name	T40-A1	T40-A1*	T40-A1**	T40-A2	T40-A3	T40-B	T40-C	T30-A1	T50-A1	
Re	430	428	427	426	429	427	429	434	421	
Type K	T_0 (K)	292.10	292.25	292.45	292.26	292.39	291.50	291.71	292.75	292.81
	T_{max} (K)	332.25	332.47	332.69	332.97	332.69	332.27	332.24	323.40	342.09
	ΔT (K)	2.26	2.26	2.26	2.54	2.14	2.38	2.14	1.73	2.75
	θ	0.056	0.056	0.056	0.062	0.053	0.058	0.053	0.056	0.056
Type T	T_0 (K)	292.10	292.25	292.40	292.28	292.41	291.55	291.70	292.69	292.76
	T_{max} (K)	332.66	332.88	333.07	333.34	333.19	332.63	332.31	323.60	342.55
	ΔT (K)	4.34	4.36	4.40	4.75	4.56	4.79	4.21	3.35	5.30
	θ	0.107	0.107	0.108	0.116	0.112	0.117	0.104	0.108	0.107

others with the same properties and from the same production charge. T40-B and T40-C from Tab. 3 are experiments with different thermocouples used and with the bottom thermocouples not glued but screwed similar to the side thermocouples through the Perspex wall. For type K, θ varies by about 0.5% while it differs by about 1.3% for type T thermocouples.

It can be concluded that the repeatability is excellent when the setup is not changes between to experimental runs. When the thermocouples are reinstalled, the measured temperature differences between short and long thermocouples is up to 1.3% in relation to the temperature step or 18% related to each other (Type K from T40-A2 and T40-C). Mainly two effects can be responsible for these differences. First, the contact between thermocouple and wall changes after the reinstallation and, therefore, also the heat conduction into the wall. The second and probably more critical influence could be the positioning of the measuring tip. As this was done manually, it is possible that the thermocouple tip positions changes with reassembling. In channels with such small dimensions (13 mm height), already a small shift of the measuring position can result in significant fluid temperature differences.

4.3 Variation of Temperature Step

Finally, the influence of the temperature step shall be investigated. Therefore, cases T30-A1, T40-A1 and T50-A1 from Tab. 3 are taken into account. It can be seen that the temperature difference ΔT changes between the experiments, but the dimensionless value only changes by 0.1%. This proves the expectation that the stem effect scales linearly with the temperature step and shows once again, that the experiments have a good repeatability, especially with an unchanged thermocouple configuration.

5 Application of Numerical Analysis

In Part I [1] of this paper, a numerical analysis is presented that allows calculating the true fluid temperature from temperature measurements that are subject to stem and inertia errors. First, the required input parameters are described. An exemplary correction is done for a long thermocouple that is assumed to not experience a stem effect. The influence of different input parameters is shown. Consequently, the second thermocouple is added in the analysis process. Stem and inertia errors are described and the parameters that mostly affect them are identified.

In the following section, the results of the analysis will be validated by comparing the obtained errors with correlations from literature and discussing them considering the uncertainties in experimental conditions and material properties.

5.1 Input parameters and sensitivity analysis

The required input parameters are time-dependent temperatures measured by a thermocouple, thermocouple material and fluid properties.

Additionally, flow conditions and installation parameters of the thermocouple need to be known.

The thermocouples are modelled by the part that is inserted in the flow field (immersion length) and the shaft embedded in the wall (wall thickness). They are divided into 100 segments, for each of which the following equation is solved:

$$\begin{aligned} & \rho c \frac{T_i^{n+1} - T_i^n}{\Delta t} A_c \Delta y \\ & = k \frac{T_{i-1}^{n+1} - 2T_i^{n+1} + T_{i+1}^{n+1}}{\Delta y} A_c \\ & + h_i^{n+1} (T_{ref,i}^{n+1} - T_i^{n+1}) A_{surf} \end{aligned} \quad (8)$$

The choice of h and T_{ref} depends on the domain adjacent to a specific segment. It can represent either convective exchange with the fluid, or conductive exchange with the wall. When the adjacent domain is the fluid, T_{ref} is the fluid temperature T_f and h is calculated by considering the Nusselt number correlation from [17] by:

$$h = 0.52 \frac{k_f}{D} Re^{0.5} Pr^{0.37} \quad (9)$$

When the respective segment is surrounded by the wall, T_{ref} is T_0 and h becomes the wall contact coefficient α_w , which is a priori unknown.

The homogenized material properties ρ, c and k are already listed in Tab. 2. The time-averaged Reynolds numbers of each experiment are listed in Tab. 3 and the air is described by the fluid properties $k_f = 0.027 \text{ W/(m K)}$ and $Pr_f = 0.707$. With the given parameters, the fluid temperature is re-calculated from the measured temperature of the long thermocouple type K of experiment T40-A1. Therefore, different values of α_w were chosen, as they cannot be determined at the same time as the fluid temperature if only a single thermocouple temperature curve is known. Figure 6 shows the results of this simulation. All curves collapse together, what means that α_w does not influence the results of the long thermocouple. This means that the connection between wall and thermocouple does not change the temperature at the thermocouple tip. The long thermocouples do therefore not experience any stem effect. Nevertheless, the calculation of the fluid temperature is helpful, as it differs significantly from the

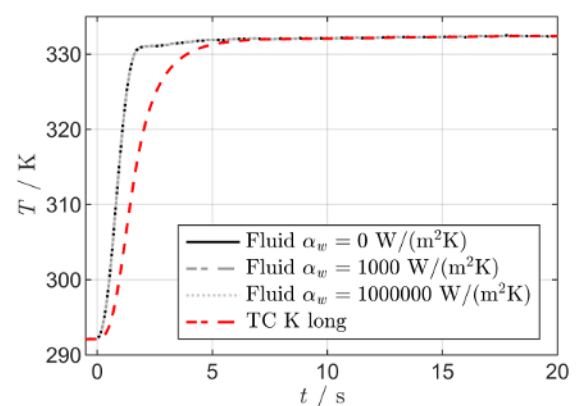


Fig. 6. Fluid temperatures re-calculated from TC K long, T40-A1, different α_w .

measured temperature data in the beginning of the experiment. These differences are due to the inertia effect of the thermocouple and will be discussed later.

When both thermocouple temperature curves are used, two fluid temperatures can be calculated. α_w is set to zero in case of the long thermocouple. For the short thermocouple, α_w is found by optimization. It is varied in the range $0 \leq \alpha_w \leq 1000$ with the criterion that the fluid temperatures re-calculated from both thermocouples match best. Figure 7 shows the results of the type K thermocouples of experiment T40-A1. The best fit of the fluid temperature curves is found with $\alpha_w = 100 \text{ W}/(\text{m}^2 \text{ K})$ for the short thermocouple. It is assumed though not proven, that the true fluid temperature is close to the re-calculated fluid temperatures. The difference between the calculated and measured temperatures can therefore be interpreted as measurement errors. They can be split into inertia errors that are present in the early phase of the experiments and stem effect errors that also appear after a long experimental duration. The inertia error is similar for both thermocouples, which was assumed as they are from the same type and dimensions. Additionally, the short thermocouple experiences a stem effect error, which can be quantified by the offset between calculated and measured fluid temperatures under quasi-stationary conditions after 20 s.

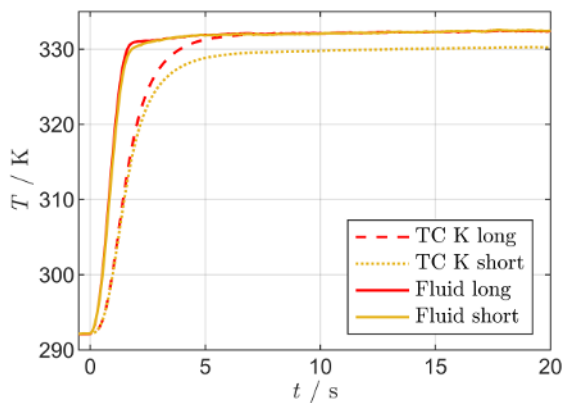


Fig. 7. Fluid temperatures re-calculated from TC K long and TC K short, T40-A1, $\alpha_w = 100 \text{ W}/(\text{m}^2 \text{ K})$.

Figure 8 shows the re-calculated fluid temperatures from the short thermocouple type K again, when $\alpha_w = 100 \text{ W}/(\text{m}^2 \text{ K})$. Now, the thermocouple properties ρc and k are varied in a range of $\pm 50\%$ and $\pm 10\%$ from the calculated values listed in Tab. 2. It is found that changing the product of density and specific heat capacity mainly affects the size of the inertia error, whereas the influence of the thermal conductivity is smaller in general and only present when the fluid already reached an almost constant level.

Additionally, in Fig. 8 the fluid temperature curves, which would have been calculated with the nominal material properties but changed wall contact coefficients, are shown. It can be seen, that by varying α_w , the re-calculated fluid temperature changes considerably. It is therefore necessary to determine α_w as accurate as possible.

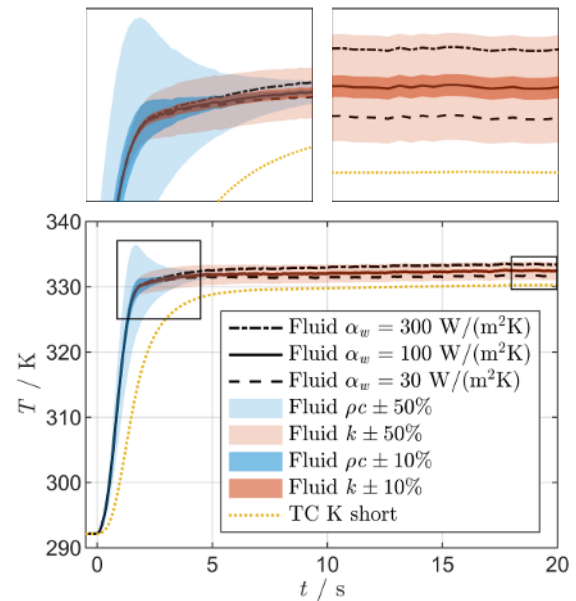


Fig. 8. Re-calculated fluid temperatures with changed thermocouple material properties, T40-A1, TC K short.

5.2 Validation

The obtained inertia and stem effects are validated separately by comparison with the simplified methods described in the introduction. In Fig. 9, the re-calculated fluid temperature from the long type K thermocouple is compared with the results of Eq. (1) when different time-constants τ are used. By inserting the given material properties and h from Eq. (9), Eq. (2) leads to $\tau = 0.84 \text{ s}$. This time constant leads to a fluid temperature curve that is almost identical to the one re-calculated by the numerical approach.

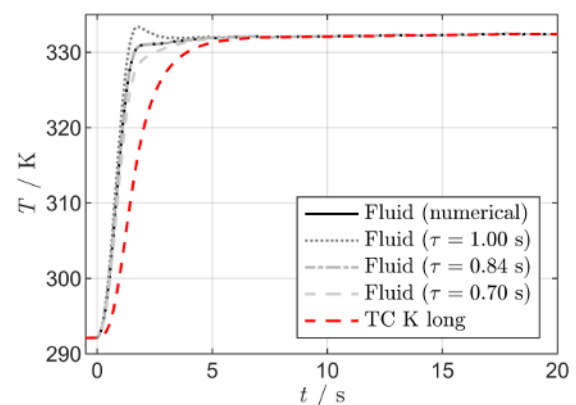


Fig. 9. Fluid temperatures re-calculated from TC K long, T40-A1, with numerical analysis and time constants.

The numerical compensation of the stem effect always depends on the wall contact parameter α_w , which is found by a curve matching between the two re-calculated fluid temperatures. Therefore, to achieve the best results in the re-calculation for the short thermocouple, a second thermocouple is needed that not experiences a stem effect. It was shown in Fig. 8, that there is no stem effect on the long thermocouple. However, the advantage of the analysis should be to allow a compensation of both the inertia and the stem effect errors, also when only one thermocouple is

available. In this case, α_w can be estimated. Therefore, the dimensionless stem effect error θ_{est} is calculated conservatively by Eq. (3) and (4) first. For both thermocouple types and their specific installation situations in this work, θ_{est} is listed in Tab. 4 and compared with the average of the experimental obtained θ (see Tab. 3). θ_{est} is then used to calculate a new true fluid temperature. By matching the re-calculated fluid temperature to that calculated with θ_{est} , the estimated wall contact coefficient α_w is found. They are listed in Tab. 5 with all α_w numerically determined from the experiments. It is found that the estimated wall contact coefficient is much higher than that based on the measurements for type K thermocouples. For type T thermocouples they are only slightly higher.

The overestimation of θ and α_w can yield a re-calculation of the fluid temperature which is more far away from the true temperature than the initially measured. Therefore, the estimation of θ should only be used when there is no possibility to have two thermocouples with different immersion lengths exposed to the same fluid temperatures. It must be clear, that the correction of the stem effect error can only be as precise as its estimation. However, it can help the experimenter to get an idea of the possible temperature error and it allows the compensation of additional inertial errors.

Better than estimating the wall contact coefficient, would be to have at least one temperature measuring position, where two thermocouples can be installed. With that a single value of α_w can be determined which can be taken for all other thermocouples of the same type and with equal installation situations. However, Tab. 5 shows that the determined α_w still varies from one situation to another.

The best application would be surely to have two thermocouples for each measuring position of which one has a high immersion length. For each measurement, the true fluid temperature could be calculated best. However, if such a configuration were possible, errors due to stem effects would not need to be compensated.

From the previous discussions of the numerical results it can be concluded, that the re-calculated fluid temperatures are reasonable and match the expectations. By activating a fast mesh heater, an almost ideal temperature step is assumed. With the given material properties, such a behaviour is observed.

5.3 Numerical Results

To highlight the importance of an accurate determination of the fluid temperature on measurement results, the measurement errors of all previously described experiments shall be quantified. As there are fluid temperatures re-calculated for both thermocouples in one position, their average is assumed to be the true fluid temperature:

$$T_f = \frac{T_{f, \text{long}} + T_{f, \text{short}}}{2} \quad (10)$$

Tab. 4. Estimated and experimental stem effect errors.

Parameter	Type K	Type T
θ_{est}	0.0888	0.1287
θ_{ave}	0.0564	0.1095

Tab. 5. Estimated and numerically determined wall contact coefficients.

α_w (W/m ² K)	Type K	Type T
estimated	510	520
T40-A1	100	350
T40-A1*	100	330
T40-A1**	100	330
T40-A2	180	390
T40-A3	100	340
T40-B	140	410
T40-C	100	270
T30-A1	130	320
T50-A1	120	280

The difference between measured and true fluid temperatures for all four instrumented thermocouples of the experiment T40-C is presented in Fig. 10. The highest differences appear at the early phase of the experiments due to the inertia of the thermocouples. The inertia effect is similar for all thermocouples. Although they are from type K and type T, respectively, the product ρc is almost identical for both types and, therefore, also the inertia effect. The stem effect is clearly seen as the shift between the temperature curves. For the short thermocouple type K, also the differences of the re-calculated temperatures to the true fluid temperatures are shown if the numerical tool worked with no wall contact coefficient and an estimated one, respectively. In these cases, the thermal inertia errors are corrected but the wrong wall contact coefficients still lead to an underestimation or overestimation of the temperature.

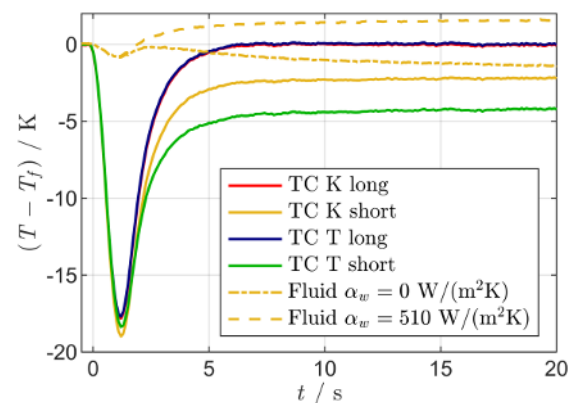


Fig. 10. Deviation from the true fluid temperature, T40-C.

Finally, it is discussed how the present temperature measurement errors would affect a transient heat transfer experiment. In a transient experiment with time-dependent fluid temperature the from a hot fluid to an isothermal wall at $T_w = T_0$ convectively transferred energy writes

$$Q = h A \int_0^t (T_f(t) - T_0) dt. \quad (11)$$

When instead of the true fluid temperature in Eq. (11) the lower measured temperature is used, the calculated transferred energy is underestimated as well. In e.g. experiments with thermochromic liquid crystals, where one-dimensional heat conduction into a semi-infinite wall is assumed, this will lead to an overestimated heat transfer coefficient h . Instead of describing the temperature difference at each time step as done in Fig. 10, now the integral temperature error is calculated by

$$e(t) = \left| 1 - \frac{\int_0^t (T(\tilde{t}) - T_0) d\tilde{t}}{\int_0^t (T_f(\tilde{t}) - T_0) d\tilde{t}} \right|. \quad (12)$$

It shows how much the convectively transferred heat is underestimated if the measured thermocouple data are trusted. The results for the experimental run T40-C are presented in Fig. 11. For all thermocouples, the error reduces with the duration of the experiment. It shall be mentioned that these error curves are still conservatively, as the wall would heat up over time in a typical experiment. This would lead to a decreasing heat transfer into the wall and a higher influence of the first seconds with extreme errors. The showed thermocouple curves are valid for all experimental settings, there are no visible differences found for the nine performed experiments. The average values of the integrated errors of the four thermocouples until times 2 s, 5 s and 20 s are listed in Tab. 6. The highest absolute deviation from a single experiments value to the corresponding average is 2%. This once again underlines the good repeatability of the conducted experiments and simulations.

Similar to Fig. 10, in Fig. 11 the errors are plotted, that would occur if the short thermocouple were corrected with the wrong wall contact coefficient α_w . The integrated error in the first seconds is much less than that of the thermocouples for which the inertia error is not corrected. After 20 s, however, the error due to the stem effect (either by neglecting or overestimation) reached a level comparable to the error due to neglect of thermal inertia.

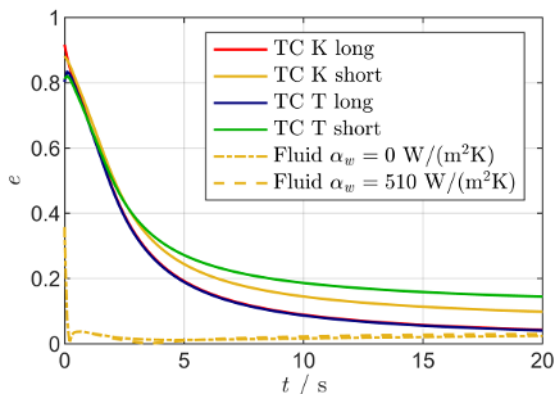


Fig. 11. Integrated temperature errors, T40-C.

Tab. 6. Average integrated temperature errors of all experiments.

	K long	K short	T long	T short
$e(t = 2 \text{ s})$	0.486	0.517	0.467	0.524
$e(t = 5 \text{ s})$	0.191	0.245	0.175	0.279
$e(t = 20 \text{ s})$	0.042	0.102	0.030	0.148

6 Conclusion

The numerical analysis presented in Part I [1] of this paper was applied to transient temperature experiments. Thermocouples with short and long immersion lengths were positioned so that they are exposed to the same fluid temperature. The repeatability of the experiments is shown for different setups and the results are similar for all of them. By applying the numerical tool, the temperature measurement errors due to both thermal inertial and the heat conduction along the thermocouple stem can be compensated. A method is proposed, that allow this compensation also if only one thermocouple with short immersion length is used. Nevertheless, it is recommended to use multiple thermocouple measures at the same position to receive most accurate fluid temperature curves. The importance of correcting these errors is demonstrated by quantifying the measurement error of a possible heat transfer experiment, where the total transferred energy from a heated fluid to an isothermal wall is extremely underestimated in the first seconds.

7 References

- [1] F. Seibold, A. Schwab, V. Dubois, R. Poser, B. Weigand, and J. von Wolfersdorf, "Conduction and Inertia Correction for Transient Thermocouple Measurements. Part I: Analytical and Numerical Modelling," *The 17th Symposium on Measuring Techniques in Transonic and Supersonic Flow in Cascades and Turbomachines*, 2020.
- [2] A. Terzis, J. von Wolfersdorf, B. Weigand, and P. Ott, "Thermocouple Thermal Inertia Effects on Impingement Heat Transfer Experiments Using the Transient Liquid Crystal Technique," *Meas. Sci. Technol.*, 2012.
- [3] F. Bernhard, *Handbuch der Technischen Temperaturmessung*, 2nd ed. Berlin: Springer Vieweg, 2014.
- [4] M. Axtmann, J. von Wolfersdorf, and G. Meyer, "Application of the Transient Heat Transfer Measurement Technique in a Low Aspect Ratio Pin Fin Cooling Channel," *Journal of Turbomachinery*, 2015.
- [5] T. Krille, S. Retzko, R. Poser, and J. von Wolfersdorf, "Heat Transfer Measurements Using Multiple Thermochromic Liquid Crystals in Symmetric Cooling Channels," *Accepted ASME Paper GT2020-16271*, 2020.
- [6] M. D. Scadron and I. Warshawsky, "Experimental Determination of Time Constants and Nusselt Numbers for Bare- Wire Thermocouples in High-Velocity Air Streams and Analytic Approximation

- of Conduction and Radiation Errors,” *NACA TN 2599*, 1952.
- [7] R. J. Dickinson, “Thermal Conduction Errors of Manganin-Constantan Thermocouple Arrays,” *Phys. Med. Biol.*, 1985.
- [8] M. Tarnopolsky and I. Seginer, “Leaf Temperature Error from Heat Conduction Along Thermocouple Wires,” *Agricultural and forest meteorology*, 1999.
- [9] K. Farahmand and J. W. Kaufman, “Experimental Measurement of Fine Thermocouple Response Time in Air,” *Experimental Heat Transfer*, 2001.
- [10] B. W. Asay, S. F. Son, P. M. Dickson, L. B. Smilowitz, and B. F. Henson, “An Investigation of the Dynamic Response of Thermocouples in Inert and Reacting Condensed Phase Energetic Materials,” *Propellants, Explosives, Pyrotechnics*, 2005.
- [11] B. Sarnes and E. Schrüfer, “Determination of the Time Behavior of Thermocouples for Sensor Speedup and Medium Supervision,” *Proc. Estonian Acad. Sci. Eng.*, 2007.
- [12] L. Villafañe and G. Paniagua, “Aero-thermal Analysis of Shielded Fine Wire Thermocouple Probes,” *International Journal of Thermal Sciences*, 2013.
- [13] M. A. Kazemi, D. S. Nobes, and J. A. W. Elliott, “Effect of the Thermocouple on Measuring the Temperature Discontinuity at a Liquid-Vapor Interface,” *Langmuir*, 2017.
- [14] Special Metals Corporation, *INCONEL® Alloy 600*. [Online]. Available: <https://www.specialmetals.com/tech-center/alloys.html>
- [15] E. D. Palik, Ed., *Handbook of Optical Constants of Solids*. Boston: Acad. Press, 2003.
- [16] S. Andersson and G. Bäckström, “Techniques for Determining Thermal Conductivity and Heat Capacity Under Hydrostatic Pressure,” *Review of Scientific Instruments*, 1986.
- [17] H. D. Baehr and K. Stephan, *Wärme- und Stoffübertragung*, 8th ed. Berlin, Heidelberg: Springer Berlin Heidelberg, 2013.